Improved back stress and synergetic strain hardening in coarse-grain/nanostructure laminates

Yanfei Wang, Muxin Yang, Xiaolong Ma, Mingsai Wang, Kun Yin, Aihui Huang, Chongxiang Huang

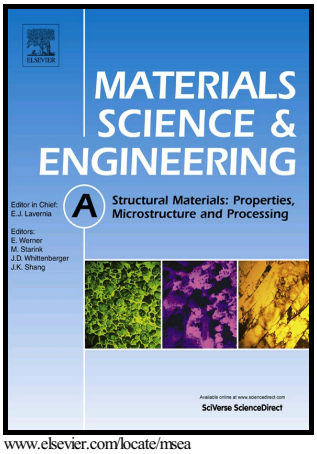

www.elsevier.com/locate/msea

PII: S0921-5093(18)30630-0
DOI: https://doi.org/10.1016/j.msea.2018.04.107
Reference: MSA36427

To appear in: *Materials Science & Engineering A*

Received date: 8 October 2017
Revised date: 25 April 2018
Accepted date: 25 April 2018

Cite this article as: Yanfei Wang, Muxin Yang, Xiaolong Ma, Mingsai Wang, Kun Yin, Aihui Huang and Chongxiang Huang, Improved back stress and synergetic strain hardening in coarse-grain/nanostructure laminates, *Materials Science & Engineering A,* https://doi.org/10.1016/j.msea.2018.04.107

Improved back stress and synergetic strain hardening in coarse-grain/nanostructure laminates

Yanfei Wang[1], Muxin Yang[2], Xiaolong Ma[3], Mingsai Wang[1], Kun Yin[1], Aihui Huang[1], Chongxiang Huang[1,*]

[1] School of Aeronautics and Astronautics, Sichuan University, Chengdu, 610065, China;
[2] State Key Laboratory of Nonlinear Mechanics, Institute of Mechanics, Chinese Academy of Sciences, Beijing 100190, China;
[3] Department of Materials Science and Engineering, North Carolina State University, Raleigh, NC 27695, USA;

* Corresponding author: Chongxiang Huang. E-mail: chxhuang@scu.edu.cn

Abstract

The effect of back stress on the mechanical behaviors of heterogeneous material is studied in two modeled heterogeneous laminates, i.e. laminated structure with a nanostructured (NS) Cu-Zn alloy layer sandwiched between two coarse-grained (CG) pure Cu layers. The improved tensile ductility of NS layer is revealed and attributed to the constraint from the stable CG layers. It is found that the elastic/plastic interaction between NS and CG layers is capable of significantly improving the back stress, which makes a significant contribution to the synergetic strain hardening in low strain stage. Furthermore, a higher mechanical incompatibility permits stronger and longer mutual interaction between layers, i.e. coupling effect, which contributes to a higher back stress. These results improve our understanding about the role of back stress on mechanical behaviors of heterogeneous laminate materials.

Keywords: laminate; back stress; strain hardening; elastic/plastic interaction; nanostructure

1. Introduction

As a new strategy for balancing or evading the strength-ductility trade-off dilemma in metallic materials, the heterogeneous structures with multiscale grain sizes, such as gradient and laminate structures, have attracted extensive interests in recent years [1-15]. It was reported that the nanostructured (NS) surface layer produced by severe plastic deformation in gradient materials could be stretched as long as its coarse-grained (CG) counterpart [3-8]. The extraordinary strain hardening and synergetic strengthening revealed in gradient IF steel were verified to be intrinsic mechanical responses for gradient materials [4,5]. In addition, the work hardening rate and tensile ductility of NS component in CG/NS laminate materials were improved simultaneously as well [12,13]. It is generally believed that the unusual dislocation multiplication, interaction and pile-up behaviors induced by complex stress/strain states in heterogeneous materials are the physical origins of above optimized properties [1,2,4-6,11].

According to the interaction between mobile dislocation and internal stress, the internal stress in materials can be divided into back stress and effective stress [16-19]. The back stress is the directional component of internal stress, i.e. long-range internal stress, which is produced by the ordered accumulation of geometrically necessary dislocations (GNDs). The effective stress is the thermal-related isotropic part of internal stress. Generally, the back stress and the effective stress can be derived from loading-unloading-reloading (LUR) loops in experiment [18-21].

During the deformation of heterogeneous materials, the strain gradient near the interface between incompatible components can be accommodated by the piling up of GNDs, which leads to a complex stress state near interface and activates more hard slip systems [4,11,12,17]. These processes play a critical role in shaping the internal stress fields, especially the development of back stress. Therefore, tracking the evolution of back stress and effective stress in heterogeneous materials would be an effective way to reveal the real-time deformation and load-bearing mechanisms. With a good prototype, the back-stress-assisted strengthening was revealed in a heterogeneous lamella pure Ti recently [11]. However, the detailed role of back stress in different straining stages and their dependence on structural parameters, such as the

level of heterogeneity across interface, are not well understood. In addition, for the purpose of optimizing structure design it is necessary to quantify the extra back stress induced by the strain gradient near a single or separated interface [2,12].

In this paper, the evolution of back stress and its contribution to strain hardening were studied in two types of heterogeneous laminates with different mechanical incompatibility. The internal stress partition mechanism and hardening process which were dominated by back stress were discussed based on the experimental results.

2. Experimental methods

Two laminated materials with a NS Cu-Zn alloy layer sandwiched between two CG pure Cu layers were fabricated by high pressure torsion, rolling and subsequent proper annealing. The detailed fabrication principles and procedures were given in our previous work [13]. The as-prepared laminates have two well-bounded interfaces.

The samples for cross-sectional optical observation were carefully polished by abrasive papers. The heterogeneous microstructure near interface was characterized by ion channeling contrast microscopy (ICCM) and transmission electron microscopy (TEM). To evaluate the cross-interface mechanical incompatibility of the processed laminates, Vickers micro-hardness was measured on the cross-section using a load of 10 g for 15 s. The dog-bone shaped tensile specimens with a gauge size of 10×1.2×0.5 mm^3 were machined from the center of disks by spark cutting. The pure NS and CG samples were peeled from laminates by polishing off other layers. Both uniaxial tension and LUR tests were performed at a strain rate of 5×10^{-4} s^{-1}. An extensometer was used to calibrate strain and each test was repeated for at least 3 samples. In order to study the influence of incompatibility level on mechanical response, we chose two types of Cu-Zn alloys as the central layer, i.e. Cu-10wt.%Zn and Cu-30wt.%Zn, and the corresponding laminates are referred to Cu-Cu10Zn-Cu and Cu-Cu30Zn-Cu, respectively.

3. Results and discussion

3.1. Heterogeneous structure

Fig. 1(a) shows a typical optical micrograph of heterogeneous laminates including the interfaces. The volume fraction of the central Cu-Zn alloy layers in Cu-Cu10Zn-Cu and Cu-Cu30Zn-Cu samples are measured as 35% and 36%, respectively. Fig. 1(b) is an ICCM image showing a significant microstructural difference across the interface. The Cu layer is characterized with fully recrystallized coarse grains, while the central Cu-Zn alloy exhibits severely deformed nanostructure (Fig. 1(c)). There is no significant difference between Cu-Cu10Zn-Cu and Cu-Cu30Zn-Cu, except for a little smaller grain size of NS Cu-30Zn layer than that of Cu-10Zn layer. As shown by the cross-sectional hardness profiles in Fig. 1(d), the abrupt transition at the interfaces of Cu-Cu10Zn-Cu and Cu-Cu30Zn-Cu are ~780MPa and ~1380MPa, respectively, while the values within each layer are rather homogenous. These indicate an obvious mechanical incompatibility between layers and are expected to raise their interaction during straining. Importantly, the discrete sharp interface in laminates is significantly different from the gradual transition microstructure in gradient materials, which provides an opportunity to quantify the mechanical effect of a single interface [4,12].

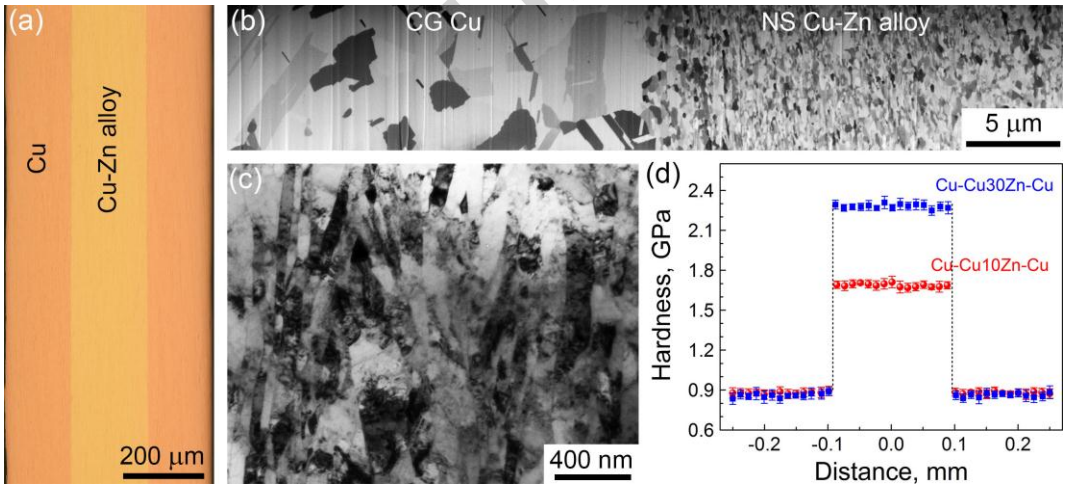

Fig. 1. Structural characteristics of CG/NS/CG laminates. (a) Optical image showing the cross-section with two straight interfaces. (b) ICCM image showing the sharp interface between CG Cu and NS Cu-Zn alloy. (c) TEM microstructure of NS Cu-Zn alloy. (d) Vickers micro-hardness profiles on the cross-section.

3.2. Improved mechanical properties

The engineering stress-strain curves of laminate samples and their component counterparts are shown in Fig. 2(a). Obviously, the laminate samples exhibit a good combination of high strength and high ductility. The uniform elongations (E_u) of Cu-Cu10Zn-Cu and Cu-Cu30Zn-Cu samples are measured as 13.5% and 11.2%, respectively. This suggests an unusual plastic deformation process activated in the central NS layers, which contributes to much higher E_u than that of their standalone NS layers (~1% for Cu10Zn, ~1.8% for Cu30Zn).

Generally, the early strain localization of bulk NS materials originates from the surface defects due to high stress concentration, and then quickly propagates across the maximum shear stress plane. The crack propagation is hard to be arrested by nano-grained microstructure, because there is almost no space for further dislocation accumulation, i.e. lack of strain hardening [22-24]. However, when the well-bonded laminates were pulled, the fast strain localization tendency of NS layer can be effectively constrained by the stable CG Cu layers through interfaces [1,14]. During the co-deformation process, the applied uniaxial stress was converted to triaxial stress state near interfaces, which activated more dislocation sources and slip systems for strain hardening. As a result, the intergranular stress concentration of NS layer was released. In addition, the strain partitioning between incompatible layers may also play an important role in relieving the strain localization as well [11,15,25].

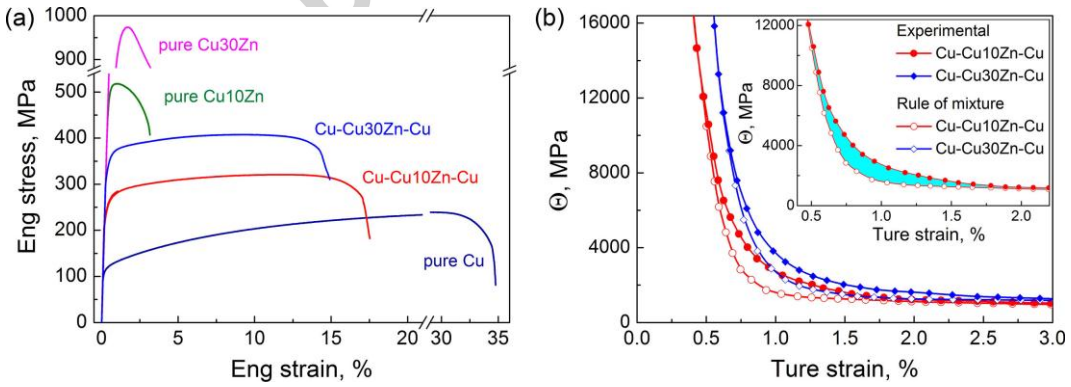

Fig. 2. (a) Uniaxial tensile stress-strain curves of CG/NS/CG laminates and their component counterparts. (b) Comparison of the strain hardening rate (Θ) of laminates between experimental results and predictions using rule-of-mixture.

The extra mechanical responses induced by the synergetic interaction between

incompatible components in heterogeneous material, such as the extra strain hardening and extra back stress, can be deduced by subtracting the rule-of-mixture prediction (ROM) from the experimentally measured results [26]. For laminate materials, the volume fraction-based ROM can be expressed as [5]:

$$f_{ROM} = \sum V_i f_i (\mathrm{i} = 1,2,3), \quad (1)$$

where f_{ROM} is the predicted result of the whole sample, V_i and f_i are the volume fraction and the mechanical parameter of component *i*, respectively. The strain hardening rate ($\Theta = d\sigma/d\varepsilon$) of CG/NS laminates was predicted based on the assumption that the central NS component keeps a constant engineering flow stress after the necking-start point of its standalone counterpart [13], as shown by the open symbols in Fig. 2(b). It is clear that the predicted strain hardening rate of either Cu-Cu10Zn-Cu or Cu-Cu30Zn-Cu samples is lower than the experimental results in low plastic strain stage, as shown by the blue shadow area in the inset of Fig. 2(b). This indicates a prominent synergetic hardening in the CG/NS heterogeneous laminates. Here, the over part of strain hardening rate than the ROM prediction is named as extra strain hardening (the shadow area in Fig. 2(b)).

3.3. Effects of back stress on mechanical properties

The LUR tests were conducted to investigate the effect of back stress on mechanical response as well as the physical origin of extra strain hardening appeared in CG/NS laminates. Fig. 3(a) shows the true LUR stress-strain curves of both pure and laminate samples. The typical hysteresis loops are compared in Fig. 3(b). It is obvious that the heterogeneous laminates have much plump hysteresis loops, suggesting stronger bauschinger effect. Fig. 3(c) shows a significant anelastic recovery strain (ε_{ae}) in the unloading process of laminates, especially the one with higher mechanical incompatibility (Cu-Cu30Zn-Cu). This would be due to the fast plastic yielding occurred during reverse loading.

The partition of back stress (σ_b) and effective stress (σ_{eff}) in unloading half cycle is schematically illustrated in Fig. 3(d). Quasi-elastic segment P_0P_1 is the thermal part of flow stress (σ^*) [18-20]. P_1P_2 is the absolute elastic stage with an effective

modulus of E_{eff}. P_3 is the reverse yield point, which is deviated from the elastic limit P_2 with a plastic strain offset equal to 0.1%, i.e. $\varepsilon_2=\varepsilon_3+0.1\%$. σ_{eff} and σ_b can be expressed as [11,18,19]

$$\sigma_{\text{eff}} = \frac{(\sigma_0 - \sigma_{rev})}{2} + \frac{\sigma^*}{2}, \tag{2}$$

and

$$\sigma_{\text{b}} = \sigma_0 - \sigma_{\text{eff}}, \tag{3}$$

where σ_0 is the flow stress.

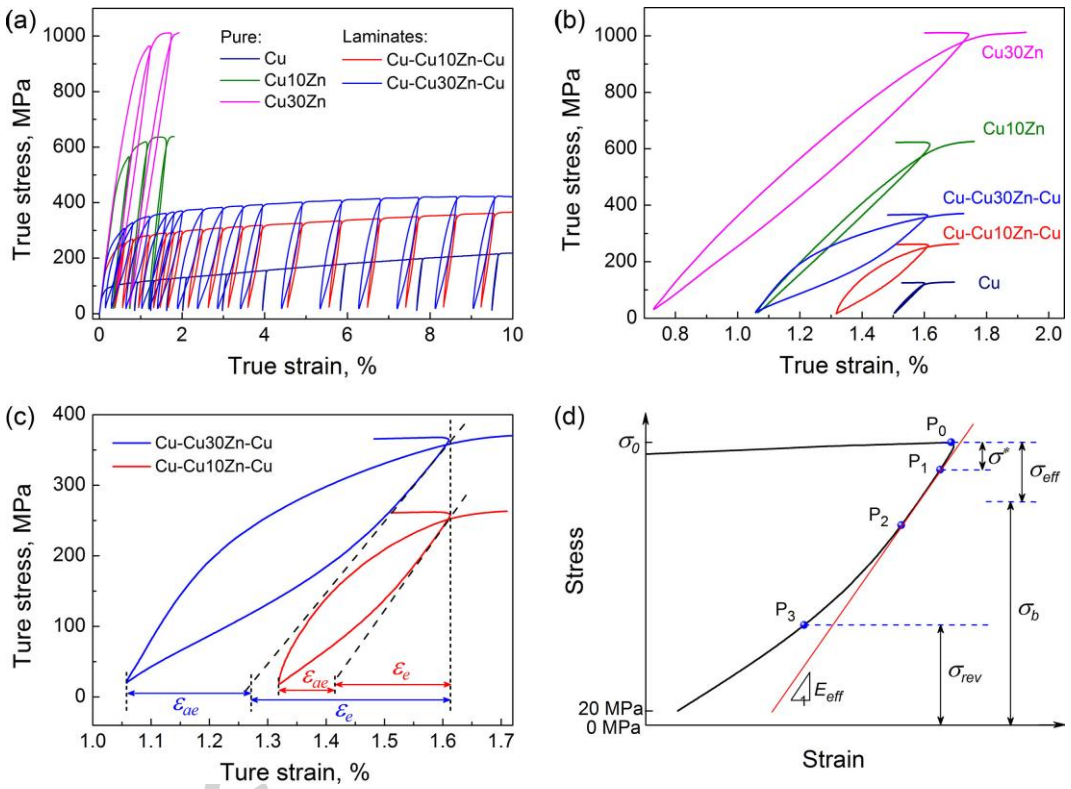

Fig. 3. Loading-unloading-reloading (LUR) tests for CG/NS/CG laminates. (a) True stress-strain curves of laminates and their pure component counterparts. (b) Comparison of the hysteresis loops. (c) The plump hysteresis loops of heterogeneous laminates showing early yielding and considerable anelastic recovery strain (ε_{ae}) during unloading. ε_e is the elastic recovery strain. (d) Schematic illustration of the partition of back stress (σ_b) and effective stress (σ_{eff}) in unloading half cycle.

Fig. 4(a) shows the evolution of back stress and effective stress of both laminate

and pure samples, which were derived from the hysteresis loops shown in Fig. 3. It is seen that the back stress increased quickly in the beginning of plastic deformation (<2%) and then slowed down as plastic strain increased. The back stress accounts for a large percentage of flow stress (σ_b/σ_0), >65% and >75% for Cu-Cu10Zn-Cu and Cu-Cu30Zn-Cu, respectively, as shown in Fig. 4(b). It should be noted that the observed high back stress in pure NS Cu-Zn samples is mainly attributed to the inhomogeneous distribution of dislocations caused by the pinning of solution atoms and the impeding of high fraction of grain boundaries [16,17,21]. However, these mechanisms can not be completely applied to NS/CG laminates, because the latter has macroscopic structural heterogeneity. For example, the extra back stress (the shadow regions in Fig. 4(b)) induced by the coupling deformation between incompatible layers accounts for a large percentage of flow stress as well. This will be derived quantitatively in the following content.

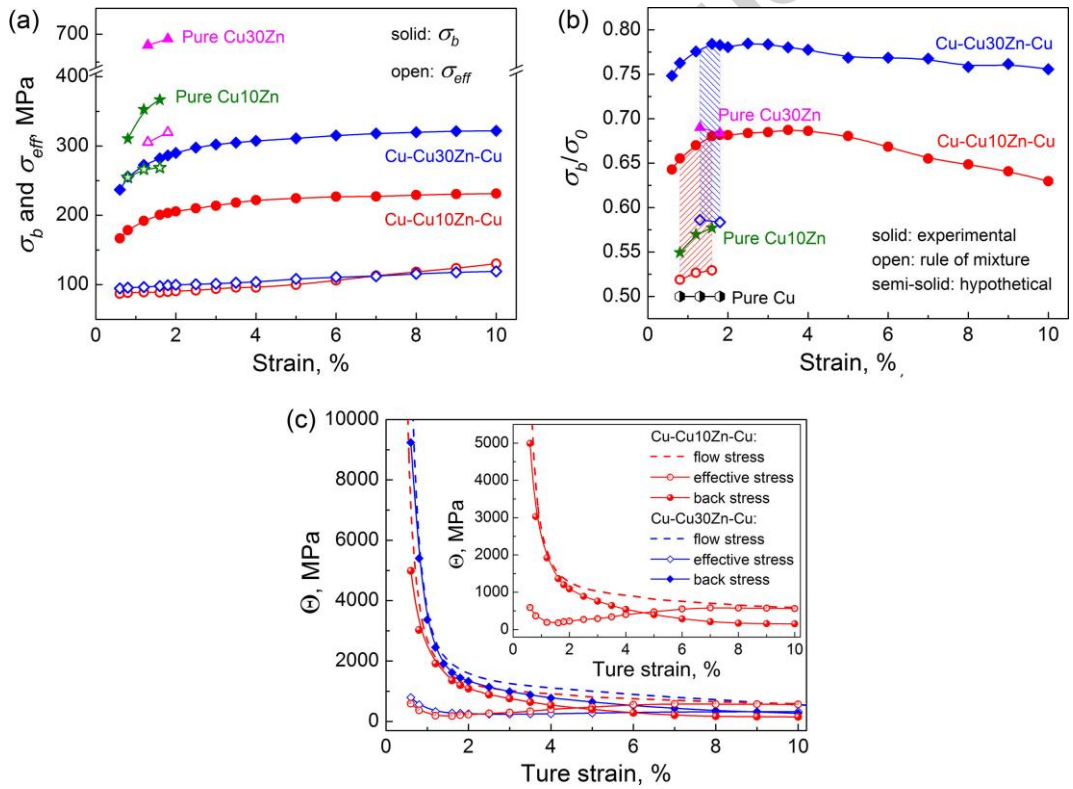

Fig. 4. (a) The evolution of back stress and effective stress of CG/NS/CG laminates and their pure component counterparts with increasing tensile strain. (b) The percentage of back stress in flow stress (σ_b/σ_0) at different strains: the solid symbols are experimental results, the open are ROM-based predictions of laminates, and the

semi-solid are the upper limit value for pure CG Cu. The shadow regions indicate the extra percentage induced by coupling interaction. (c) Strain hardening rate (Θ) of the flow stress, back stress and effective stress of laminates with increasing applied strain.

The large difference of elastic limit between pure CG Cu (~0.08%) and NS Cu-Zn alloy (~0.45% for Cu10Zn, ~0.82% for Cu30Zn) provides heterogeneous laminates a long stage of elastic-plastic transition, during which the dislocations-dominated fast shrinking of yielded CG Cu is restricted by the lateral tensile stress from elastic NS layer. This process can not only contribute directly to improve the yield strength of laminates, but also introduce great strain gradient near interfaces, which is accommodated by ordered accumulation of GNDs [11,12,27,28]. Accordingly, the back stress increases quickly with accumulating strain gradient, which demands higher external shear stress for further nucleation and propagation of dislocations. However, on the other hand it acts as driving force for the dissolution and reverse motion of unstable dislocations during unloading process [17,18,29]. The effective stress increases slowly because of limited motion of mobile dislocations in this stage [4,19]. Therefore, it is the back stress that controls the variety of strain hardening rate in low strain stage, as shown in Fig. 4(c).

There is no obvious reverse yielding point for CG Cu even unloaded to 0 MPa, so that the back stress cannot be calculated using Equations (2) and (3) [19,30]. To quantify the extra back stress component ($\sigma_{b,coupling}$) induced by above coupling deformation process in heterogeneous laminates, it is needed to assume that CG Cu yields at 0 MPa during unloading, namely, the back stress accounts for about 50% of the flow stress. This assumption provides the upper limit of the back stress for CG Cu. In this way a conservative calculation of $\sigma_{b,coupling}$ can be expressed as

$$\sigma_{b,coupling} = \sigma_{b,physical} - \sigma_{b,ROM}, \quad (4)$$

where $\sigma_{b,physical}$ is the back stress of experiment sample (Fig. 4(a)), $\sigma_{b,ROM}$ is the back stress calculated using the ROM (Equation (1)). It is surprising that the $\sigma_{b,coupling}$ of Cu-Cu10Zn-Cu and Cu-Cu30Zn-Cu laminate samples accounts for about 14% and 20% of the flow stress, respectively, as shown by the shadow regions in Fig. 4(b). This

indicates that the synergetic strengthening and hardening in heterogeneous materials are realized through the development of back stress. Therefore, it is reasonable to believe that the high value of extra back stress is the origin for the extra strain hardening observed in experiment laminates (Fig. 2(b)) [11,12,27].

When the strain gradient near interfaces was built up gradually with increasing tensile strain, the increase of back stress slowed down, as shown in Fig. 4. However, the value of back stress still kept at a high level in the high strain stage, indicating a sustained interaction between CG and NS layers. Fig. 5 shows the typical fracture surface of a laminate sample. It is seen that the dimples in NS layer aligned up and coalesced in the tensile direction, while the dimples in CG layer elongated perpendicular to the interface. This fracture mode provides a powerful evidence to verify the strong lateral constraint between NS and CG layers in the high plastic strain stage.

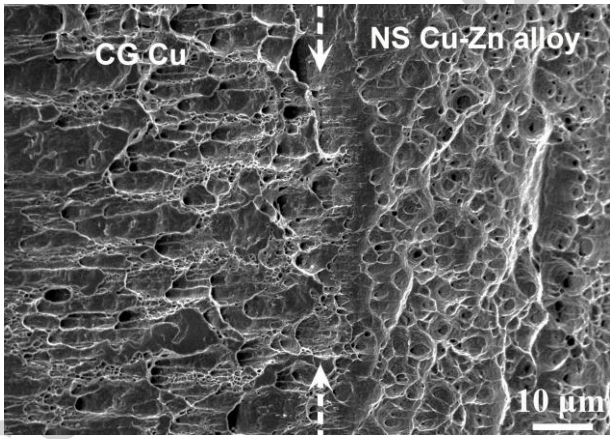

Fig. 5. Typical fracture surface across the interface of CG/NS/CG laminates. The white dotted arrows mark the position of interface.

In heterogeneous material, higher mechanical heterogeneity between components can result in a stronger and longer coupling process. It is reasonable that the $\sigma_{b,coupling}/\sigma_0$ of Cu-Cu30Zn-Cu laminate is higher than that of Cu-Cu10Zn-Cu laminate, because the former has higher hardness gradient across interface and therefore longer elastic-plastic transition stage.

On the other hand, a high level of back stress could activate some harder slip

systems in CG and NS components [11,17], and therefore promote the nucleation and entanglement of dislocations, which resulted in a fast increase of effective stress as well as its strain hardening rate in the high strain stage, as shown in Fig. 4(a) and (c). As for the lower increasing rate of effective stress in Cu-Cu30Zn-Cu compared with that in Cu-Cu10Zn-Cu laminate at high strain, the possible reason is that the higher mechanical incompatibility would cause more serious stress concentration at interface, which is prone to resulting in relatively earlier damaging tendency and lower strain hardening rate in the late stage of plastic deformation.

Note that the observed high back stress and extraordinary strain hardening are originated from the coupling effect around two discrete interfaces, which needs the ordered piling-up of GNDs near interface [12]. Higher density of interface in heterogeneous laminates is expected to maximize the GNDs piling-up as well as the back stress [2]. However, the extremely high interface density in multilayers with very small layer thickness may change the dislocation interaction mechanisms [31], which can not be explained by current mechanism of GNDs piling-up near interface. Besides, the sharp interface with excessive mechanical incompatibility level may cause stress singularities, such as micro-cracks and voids at interface during straining, and deteriorate the interaction on the contrary. Therefore, there would be optimum interface density, arrangement and incompatibility level of heterogeneous laminates for the maximum back stress and synergetic strength.

4. Conclusions

In summary, the effect of back stress on the mechanical properties of CG/NS/CG laminate materials was quantitatively studied by uniaxial and LUR tensile tests. The conclusions can be summarized as below:

(1) A synergetic strain hardening was revealed in the low strain stage of heterogeneous laminates, which contributed to the improvement of the tensile ductility of NS layer.

(2) The extra back stress induced by elastic/plastic interaction at the two discrete interfaces of Cu-Cu10Zn-Cu and Cu-Cu30Zn-Cu laminates accounted for about 14%

and 20% of flow stress, respectively, which was the origin of the extra strain hardening appeared in heterogeneous laminates.

(3) Both higher mechanical incompatibility across interface and longer elastic-plastic interaction process are expected to produce a higher back stress. However, excessive mechanical incompatibility between layers may cause stress singularities and thus weaken the interaction. There would be an optimal incompatibility level between layers for the maximum back stress and synergetic strength.

Acknowledgements

This work was supported by the National Natural Science Foundation of China (No.11672195, No.51601204) and Sichuan Youth Science and Technology Foundation (2016JQ0047).

Reference

[1] K. Lu, Making strong nanomaterials ductile with gradients, Science 345 (2014) 1455-1456.

[2] X.L. Wu, Y.T. Zhu, Heterogeneous materials: a new class of materials with unprecedented mechanical properties, Mater. Res. Lett. 5 (2017) 527-532.

[3] T.H. Fang, K. Lu, Revealing extraordinary intrinsic tensile plasticity in gradient nano-grained copper, Science 331(2011)1578-1590.

[4] X.L. Wu, P. Jiang, L. Chen, F.P. Yuan, Y.T. Zhu, Extraordinary strain hardening by gradient structure, Proc. Natl. Acad. Sci. U.S.A. 111 (2014) 7197–7201.

[5] X.L. Wu, P. Jiang, L. Chen, J.F. Zhang, F.P. Yuan, Y.T. Zhu, Synergetic strengthening by gradient structure, Mater. Res. Lett. 2 (2014) 185–191.

[6] J.J. Li, G.J. Weng, S.H. Chen, X.L. Wu, On strain hardening mechanism in gradient nanostructures, Int. J. Plasticity. 88 (2017) 89-107.

[7] B.C. Zhu, X.L. Ma, J. Moering, H. Zhou, X.C. Yang, X.K. Zhu, Enhanced mechanical properties in Cu–Zn alloys with a gradient structure by surface mechanical attrition treatment at cryogenic temperature, Mater. Sci. Eng. A 626 (2015) 144–149.

[8] Z. Yin, X.C. Yang, X.L. Ma, J. Moering, J. Yang, Y.L. Gong, Y.T. Zhu, X.K. Zhu, Strength and ductility of gradient structured copper obtained by surface mechanical attrition treatment, Mater. Des. 105 (2016) 89–95.

[9] X.L. Wu, M.X. Yang, F.P. Yuan, L. Chen, Y.T. Zhu, Combining gradient structure and TRIP effect to produce austenite stainless steel with high strength and ductility, Acta Mater. 112 (2016) 337-346.

[10] Y.J. Wei, Y.Q. Li, L.C. Zhu, Y. Liu, X.Q Lei, G. Wang, Y.X. Wu, Z.L. Mi, J.B. Liu, H.T. Wang, H.J. Gao, Evading the strength–ductility trade-off dilemma in steel through gradient hierarchical nanotwins, Nat. Commun. 5 (2014) 1-8.

[11] X.L. Wu, M.X. Yang, F.P. Yuan, G.L. Wu, Y.J. Wei, X.X. Huang, Y.T. Zhu, Heterogeneous lamella structure unites ultrafine-grain strength with coarse-grain ductility, Proc. Natl. Acad. Sci. U.S.A. 112 (2015) 14501-14505.

[12] X.L. Ma, C.X. Huang, J. Moering, M. Ruppert, H. Höppel, M. Göken, J. Narayan, Y.T. Zhu, Mechanical properties of copper/bronze laminates: role of interfaces, Acta Mater. 116 (2016) 43-52.

[13] X.L. Ma, C.X. Huang, W.Z. Xu, H. Zhou, X.L. Wu, Y.T. Zhu, Strain hardening and ductility in a coarse-grain/nanostructure laminate material, Scr. Mater. 103 (2015) 57-60.

[14] A.Y. Chen, D.F. Li, J.B. Zhang, H.W. Song, J. Lu, Make nanostructured metal exceptionally tough by introducing non-localized fracture behaviors, Scr. Mater. 59 (2008) 579-582.

[15] M. Huang, G.H. Fan, L. Geng, G.J. Cao, Y. Du, H. Wu, T.T. Zhang, H.J. Kang, T.M. Wang, G.H. Du, H.L. Xie, Revealing extraordinary tensile plasticity in layered Ti-Al metal composite, Sci. Rep. 6 (2016) 38461.

[16] M.E. Kassner, P. Geantil, L.E. Levine, Long range internal stresses in single-phase crystalline materials, Int. J. Plasticity. 45 (2013) 44–60.

[17] M.F. Ashby, The deformation of plastically non-homogeneous materials, Philos. Mag. 21 (1970) 399-424.

[18] J.L. Dickson, J. Boutin, L. Handfield, A comparison of two simple methods for measuring cyclic internal and effective stresses, Mater. Sci. Eng. 64 (1984) L7-L11.

[19] X. Feaugas, On the origin of the tensile flow stress in the stainless steel AISI 316L at 300 k: back stress and effective stress, Acta Mater. 47 (1999) 3617-3632.

[20] P.S. De, A. Kundu, P.C. Chakraborti, Effect of prestrain on tensile properties and ratcheting behavior of Ti-stabilised interstitial free steel, Mater. Des. 57 (2014) 87-97.

[21] H. Haddou, M. Risbet, G. Marichal, X. Feaugas, The effects of grain size on the cyclic deformation behaviour of polycrystalline nickel, Mater. Sci. Eng. A 379 (2004) 102-111.

[22] M.A. Meyers, A. Mishra, D.J. Benson, Mechanical properties of nanocrystalline materials, Prog. Mater. Sci. 51 (2006) 427-556.

[23] C.X. Huang, W.P. Hu, Q.Y. Wang, C. Wang, G. Yang, Y.T. Zhu, An ideal ultrafine-grained structure for high strength and high ductility, Mater. Res. Lett. 3 (2015) 88-94.

[24] Y.Z. Chen, X.Y. Ma, X.H. Shi, T. Suo, C. Borchers, K.H. Zhang, F. Liu, R. Kirchheim, Hardening effects in plastically deformed Pd with the addition of H, Scr. Mater. 98 (2015) 48-51.

[25] G.H. Fan, L. Geng, H. Wu, K.S. Miao, X.P. Cui, H.J. Kang, T.M. Wang, H.L. Xie, T.Q. Xiao, Improving the tensile ductility of metal matrix composites by laminated structure: A coupled X-ray tomography and digital image correlation study, Scr. Mater. 135 (2017) 63-67.

[26] Y.F. Wang, C.X. Huang, M.S. Wang, Y.S. Li, Y.T. Zhu, Quantifying the synergetic

strengthening in gradient material, Scr. Mater. 150 (2018) 22-25.

[27] C.X. Huang, Y.F. Wang, X.L. Ma, S. Yin, H.W. Höppel, M. Göken, X.L. Wu, H.J. Gao, Y.T. Zhu, Interface affected zone for optimal strength and ductility in heterogeneous laminate, Mater. Today (2018), https://doi.org/10.1016/j.mattod.2018.03.006

[28] H. Murghrabi, On the current understanding of strain gradient plasticity, Mater. Sci. Eng. A 387 (2004) 209-213.

[29] J. Rajagopalan, C. Rentenberger, H.P. Karnthaler, G. Dehm, M.T.A. Saif, In situ TEM study of microplasticity and Bauschinger effect in nanocrystalline metals, Acta mater. 58 (2010) 4772-4782.

[30] J.K. Mahato, P.S. De, A. Sarkar, A. Kundu, P.C. Chakraborti, Effect of deformation mode and grain size on Bauschinger behavior of annealed copper, Int. J. Fatigue 83 (2016) 42–52.

[31] J. Wang, A. Misra, An overview of interface-dominated deformation mechanisms in metallic multilayers, Curr. Opin. Solid. St. M. 15 (2011) 20–28.